Endothelial progenitor cell-derived extracellular vesicles protect from complement-mediated mesangial injury in experimental anti-Thy1.1 glomerulonephritis

Cantaluppi, Vincenzo; Medica, Davide; Mannari, Claudio; Stiaccini, Giulia; Figliolini, Federico; Dellepiane, Sergio; Quercia, Alessandro Domenico; Migliori, Massimiliano; Panichi, Vincenzo; Giovannini, Luca; Bruno, Stefania; Tetta, Ciro; Biancone, Luigi; Camussi, Giovanni. Endothelial progenitor cell-derived extracellular vesicles protect from complement-mediated mesangial injury in experimental anti-Thy1.1 glomerulonephritis. NEPHROLOGY DIALYSIS TRANSPLANTATION. 30 (3) pp: 410-422.
DOI: 10.1093/ndt/gfu364

Endothelial progenitor cell-derived extracellular vesicles protect from complement-mediated mesangial injury in experimental anti-Thy1.1 glomerulonephritis

Vincenzo Cantaluppi, Davide Medica, Claudio Mannari, Giulia Stiaccini, Federico Figliolini, Sergio Dellepiane, Alessandro Domenico Quercia, Massimiliano Migliori, Vincenzo Panichi, Luca Giovannini, Stefania Bruno, Ciro Tetta, Luigi Biancone, Giovanni Camussi

Abstract

Background Endothelial progenitor cells (EPCs) are known to induce tissue repair by paracrine mechanisms including the release of growth factors and extracellular vesicles (EVs), nanoparticles able to carry proteins and genetic information to target cells. The aim of this study was to evaluate whether EVs derived from EPCs may protect from complement-mediated mesangial injury in experimental anti-Thy1.1 glomerulonephritis.

Methods EVs were isolated by serial ultracentrifugation from supernatants of cultured human EPCs and characterized for their protein and RNA content. *In vivo*, EVs were injected i.v. in the experimental rat model of mesangiolytic anti-Thy1.1 glomerulonephritis evaluating renal function, proteinuria, complement activity and histological lesions. *In vitro*, the biological effects of EPC-derived EVs were studied in cultured rat mesangial cells incubated with anti-Thy1.1 antibody and rat or human serum as complement source.

Results After i.v. injection in Thy1.1-treated rats, EVs localized within injured glomeruli and inhibited mesangial cell activation, leucocyte infiltration and apoptosis, decreased proteinuria, increased serum complement haemolytic activity (CH50) and ameliorated renal function. EV treatment decreased intraglomerular deposition of the membrane attack complex (MAC or C5b-9) and expression of smooth muscle cell actin and preserved the endothelial antigen RECA-1 and the podocyte marker synaptopodin. The protective effect of EVs was significantly reduced by pre-treatment with a high dose of RNase (1 U/mL), suggesting a key role for EV-carried RNAs in these mechanisms. Indeed, EPC-derived EVs contained different mRNAs coding for several anti-apoptotic molecules and for the complement inhibitors Factor H, CD55 and CD59 and the related proteins. The *in vitro* experiments aimed to investigate the mechanisms of EV protection indicated that EVs transferred to mesangial cell mRNAs coding for Factor H, CD55 and CD59 and inhibited anti-Thy1.1 antibody/complement-induced apoptosis and C5b-9/C3 mesangial cell deposition.

Conclusions EVs derived from EPCs exert a protective effect in Thy1.1 glomerulonephritis by inhibition of antibody- and complement-mediated injury of mesangial cells.

INTRODUCTION

Thy1.1 glomerulonephritis is characterized by complement-mediated mesangial cell injury and endothelial cell loss [1]. Several studies addressed the role of bone marrow-derived stem cells in the repair of injured glomeruli [2, 3]. Endothelial progenitor cells (EPCs) circulating bone marrow-derived precursors are able to localize within sites of vascular injury. EPCs exert protective effects in experimental models of myocardial infarction and hind limb ischaemia [4]. In Thy1.1 nephritis, intra-renal injection of EPCs was shown to reduce endothelial injury and mesangial cell activation [5]. The regenerative effect of EPCs has also been ascribed to paracrine mechanisms including the release of growth factors and of extracellular vesicles (EVs) [6, 7]. EVs include exosomes and shedding vesicles that have been recently shown to play a key role in the intercellular cross-talk through the transfer of proteins and genetic information [8]. We previously showed that EVs released from EPCs activated angiogenesis by horizontal transfer of mRNAs [7] and protected the kidney from ischaemic acute injury by delivering pro-angiogenic microRNAs [9].

The aim of this study was to evaluate whether EPC-derived EVs may have a protective effect in anti-Thy1.1 glomerulonephritis through RNA transfer to injured mesangial cells.

MATERIALS AND METHODS

Isolation and characterization of EPCs and EPC-derived EVs

EPCs were isolated and characterized from peripheral blood mononucleated cells of healthy donors by density centrifugation [7, 9]. EVs were obtained from supernatants of EPCs [10]. EV shape and size were evaluated by transmission electron microscopy and Nanosight analysis [9]. The expression of Factor H, CD55 and CD59 both in EPCs and EVs were studied by fluorescent activated cell sorter (FACS), western blot and confocal microscopy. RNA was extracted from EPCs and EVs by the mirVana isolation kit (Ambion, Austin, TX) and analysed by Agilent 2100 Bioanalyzer (Agilent Tech. Inc., Santa Clara, CA). Nucleic acid content of EVs was studied by GUAVA FACS analysis using acridine orange (Sigma Aldrich, St Louis, MO) [11]. Reverse Transcription Polymerase Chain Reaction (RT-PCR) was performed by the High-Capacity cDNA Reverse Transcription Kit (Applied Biosystems, Foster City, CA). Sequence-specific oligonucleotide primers were designed using Primer Express (Applied Biosystems); human Factor H: forward, 5'-TTACTGGGATCACATTCATTGCA-3'; reverse, 5'-TGGCAGGCAACGTCTATAGATTT-3'; human CD55: forward, 5'-TTGAAGAGTTCTGCAATCGTAGCT-3'; reverse, 5'-CTGTAACCTGGACGGCACTCAT-3'; human CD59: forward, 5'-TCTTCTGCCATTCAGGTCATAGC-3'; reverse, 5'-TGGTAATGAGACACGCATCAAAA-3'. The relative expression of different mRNAs was detected by SYBR green method using relative Ct quantification analysis (Ct = Ct target – Ct control). In selected experiments, EVs were labelled with the red fluorescent dye PKH26 (Sigma Aldrich) or treated with a high dose (1 U/mL) of RNase (Ambion) for 1 h at 37°C. Bioanalyzer and quantitative RT-PCR (qRT-PCR) were used to evaluate the total RNA content and the presence of selected mRNAs (Factor H, CD55 and CD59) and microRNAs (miR-126, miR-296) in unstimulated or RNase-treated EVs. EVs isolated from human fibroblasts were used as control in all experiments.

Experimental anti-Thy1.1 glomerulonephritis: functional and histological studies

Animal care and treatment were conducted in conformity with the National Institutes of Health Guide for animal care. Briefly, 8-week-old female Wistar rats were subjected to i.v. injection (femoral vein) of 0.5 mL of 0.9% saline containing vehicle alone or 400 μg of anti-Thy1.1 antibody (Cedarlane, Ontario, Canada). At Day 2 after anti-Thy1.1 injection, animals were divided as follows: (i) control (untreated); (ii) Thy1.1 (Thy1.1 + 0.9% saline); (iii) Thy1.1 + EPC EVs (Thy1.1 + 30 μg/100 g body weight EPC EVs); (iv) Thy1.1 + EPC EV RNase (Thy1.1 + 30 μg/100 g body weight EPC EVs pre-treated with 1 U/mL RNase) and (v) Thy1.1 + fibroblast EVs (Thy1.1 + 30 μg/100 g body weight EVs derived from human fibroblasts). Ten animals for each group were housed in ventilated cages and sacrificed after 4, 8 and 14 days. Proteinuria was measured daily on 24-h urine by an automated method (Bio-Rad Laboratories GmbH, München, Germany). Serum and urine creatinine were determined by commercially available optical densitometric kits (Arbor Assays, Ann Arbor, MI). For histological analysis, 5 μm-thick paraffin kidney sections were stained with haematoxylin and eosin stain (H&E; Merck, Darmstadt, Germany) to define the percentage of glomeruli affected by the following typical alterations: pre-ballooning, ballooning, mesangiolysis, microaneurysms, podocyte bridging and tuft adhesion [12]. Morphology of the glomerular filtration barrier was also evaluated by transmission electron microscopy [13]. Terminal deoxynucleotidyl transferase dUTP nick end labeling (TUNEL) assay (Chemicon Int., Temecula, CA) for the detection of apoptotic cells was performed. Leucocyte infiltration was evaluated by immunoperoxidase staining with an anti-monocyte (Chemicon Int.) or anti-granulocyte (Serotec, Oxford, UK) antibody. The expansion of mesangial areas was quantified by immunoperoxidase staining with an anti-smooth muscle cell actin (SMA) antibody (Dako, Glostrup, Denmark). Confocal microscopy analysis was performed on frozen sections to evaluate the expression of synaptopodin (Progen Biotechnik, Heidelberg, Germany), RECA-1 (Serotec) or C5b-9 (Santa Cruz Biotech, Santa Cruz, CA) and to evaluate biodistribution of PKH26 red-labelled EVs 2 h after injection. Complement haemolytic activity (CH50) on rat sera was evaluated by Enzyme-Linked ImmunoSorbent Assay (ELISA) (Bioassay Technology Laboratory, Shanghai, China).

Rat and human glomerular cell isolation, characterization and culture

Rat mesangial cells (RMCs) were purchased from ATCC (Manassas, VA, USA) and cultured in DMEM medium with 4 mM l-glutamine and 15% fetal bovine serum. Primary cultures of human mesangial cells, glomerular endothelial cells (GECs) and podocytes were isolated from glomeruli as previously described [14, 15].

In vitro internalization of EPC-derived EVs into different glomerular cells

RMCs, human mesangial cells, endothelial cells or podocytes were seeded on six-well plates and incubated with different doses of PKH26-labelled EVs for 2 h. EV internalization was evaluated by confocal microscopy (Zeiss LSM 5 PASCAL, Jena, Germany) or FACS in the presence or absence of 1 μg/mL of different blocking antibodies directed to αVβ3-integrin (BioLegend), α4-integrin, α6-integrin (Chemicon Int.), CD29, L-selectin (Becton Dickinson) or control irrelevant cytokeratin 19 (Dako) [9].

In vitro studies on RMCs

We recreated *in vitro* the complement-mediated damage of RMC culturing cells in the presence of anti-Thy1.1 antibody for 1 h in serum-free Roswell Park Memorial Institute medium at 37°C and with the subsequent addition of a lytic dose (33%) of normal rat or human AB serum as complement source for 40 min at 37°C [16]. After complement activation, the effects of EVs on RMCs were evaluated by the following assays.

Cell damage

RMCs (5×10^4) were cultured on 24-well and incubated with different stimuli and 250 μg/mL 2,3-bis-(2-methoxy-4-nitro-5-sulfophenyl)-2H-tetrazolium-5-carboxanilide (XTT) (Sigma Aldrich). Samples were analysed in an automatized ELISA reader at a wavelength of 450 nm [17].

Cell death

RMCs were subjected to TUNEL assay (Chemicon Int.) and analysed under a fluorescence microscope to detect green-stained apoptotic cells in 10 non-consecutive microscopic fields [18, 19]. The same samples were analysed by MUSE assay to detect the co-staining for Annexin V and 7-aminoactinomycin D (7-AAD) [20, 21].

RT-PCR, immunofluorescence and FACS studies

After incubation with anti-Thy1.1 + normal rat serum and different types of EVs, total RNA was extracted from RMCs to perform RT-PCR for human Factor H, CD55 and CD59. RMCs were stained with specific antibodies directed to rat or human C5b-9 (Santa Cruz or Dako, respectively), C3, Factor H (Abcam), CD55 or CD59 (Becton Dickinson): cells were then incubated with appropriated fluorescein isothiocyanate or phycoerythrin conjugated secondary anti-IgG antibodies and examined by immunofluorescence and FACS.

Statistical analysis

All data of different experimental procedures are expressed as average ± SD. Statistical analysis was performed by Student's *t*-test or ANOVA with the Newman–Keuls multicomparison test. For FACS, the Kolmogorov–Smirnov nonparametric statistical test was performed.

RESULTS

Characterization of EPC-derived EVs and expression of complement inhibitors

Purified EVs showed a homogenous pattern of spheroid particles with a size ranging from 60 to 130 nm as seen by electron microscopy and confirmed by Nanosight analysis (Figure S1A, Supplementary Material). Acridine orange staining showed that EVs derived from EPCs were positive for RNA but negative for DNA (Figure S1B, Supplementary Material). We found by RT-PCR that EPCs expressed mRNAs coding for the complement inhibitors Factor H, CD55 and CD59 (Figure 1A). The expression of these complement inhibitors was confirmed at the protein level in EPCs by FACS and immunofluorescence studies (Figure 1B). EPC-derived EVs carried both mRNAs coding for Factor H, CD55 and CD59 (Figure 1A) and the related proteins (western blot and FACS analysis in Figure 1C and D, respectively). Treatment of EPC-derived EVs with high doses of RNase (1 U/mL) decreased the RNA content of EVs (Figure S1C, Supplementary Material), including the mRNAs coding for Factor H, CD55 and CD59 and microRNAs involved in angiogenesis such as miR-126 and miR-296 (Figure S1D, Supplementary Material) [7, 9].

FIGURE 1

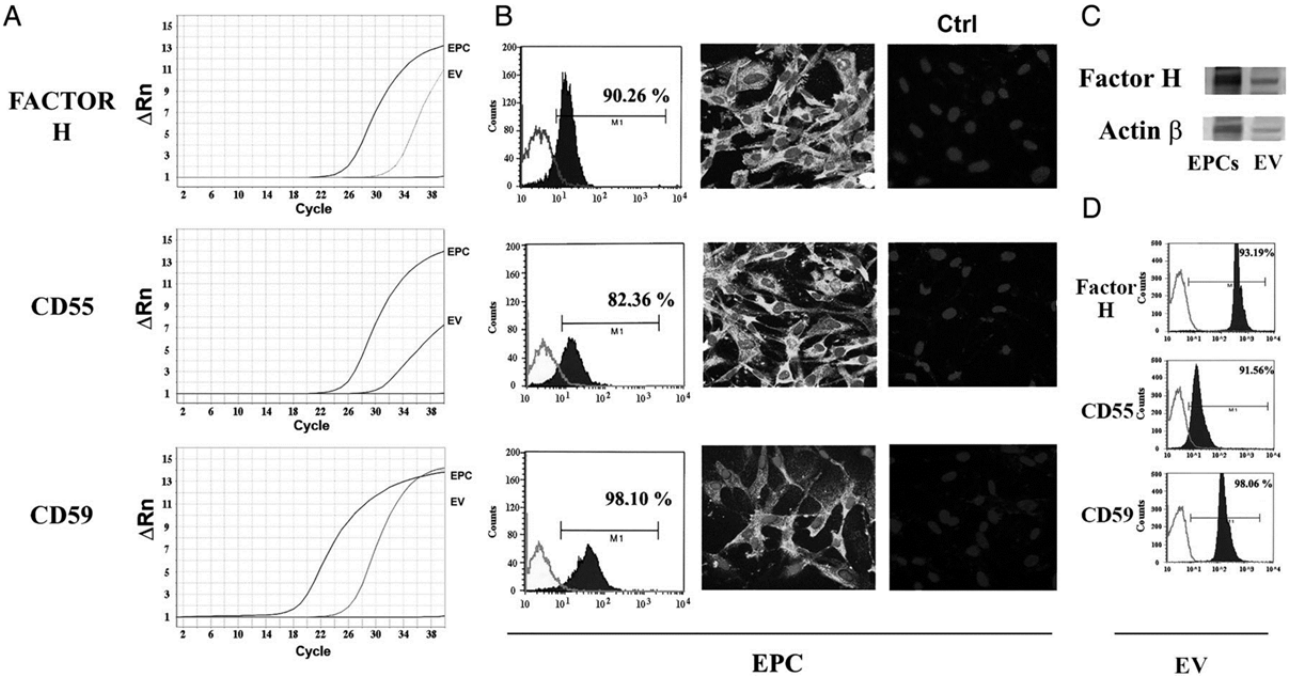

Expression of complement inhibitors Factor H, CD55 and CD59 by EPCs and EPC-derived EVs. (**A**) Representative qRT-PCR showing the expression of mRNAs coding for Factor H, CD55 and CD59 in both EPCs and EPC-derived EVs (left panels). (**B**) FACS and confocal microscope analysis showing Factor H, CD55, CD59 expression in EPCs (EPC, central panels). (**C** and **D**) Western blotting (C, EPC was used as control) and FACS analysis (D) detecting Factor H, CD55, CD59 in EPC-derived EVs (EV, right panels). For FACS analysis, control-matched isotype was used as experimental control (open curves). Kolmogorov–Smirnov statistical analysis was performed. For western blot analysis of Factor H, α-actin was used as positive control. Three independent experiments were performed with similar results.

EPC-derived EVs reduced proteinuria and preserved renal function in anti-Thy1.1 nephritis

We evaluated the effects of EPC-derived EVs in the experimental model of anti-Thy1.1-induced glomerulonephritis (Figure 2). In the Thy1.1 group, proteinuria significantly rose at Day 2–3, peaked at Day 8–10 and then progressively decreased (Figure 3A). EPC-derived EVs significantly decreased proteinuria at all time points observed. The anti-proteinuric effect of EVs was abated after pre-treatment with 1 U/mL RNase (Figure 3A). The most relevant difference between the experimental groups was observed at Day 8 (Figure 3A and B). The protective effect was specific for EPC-derived EVs, because EVs released from human fibroblasts were ineffective (Figure 3B). This was associated with a different RNA content of fibroblast-derived EVs. Indeed, EVs released from fibroblasts showed a size and a concentration similar to those of EPC-derived EVs (Figure S2A, Supplementary Material), but they did not express Factor H, CD55 and CD59 at both gene and protein level, despite these mRNAs being slightly expressed by the cells of origin (Figure S2B and C, Supplementary Material). Administration of EPC-derived EVs preserved renal function as shown

by creatinine clearance (Figure 3C). This effect was not observed using RNase-treated EPC-derived EVs or EVs released from human fibroblasts (Figure 3C).

FIGURE 2

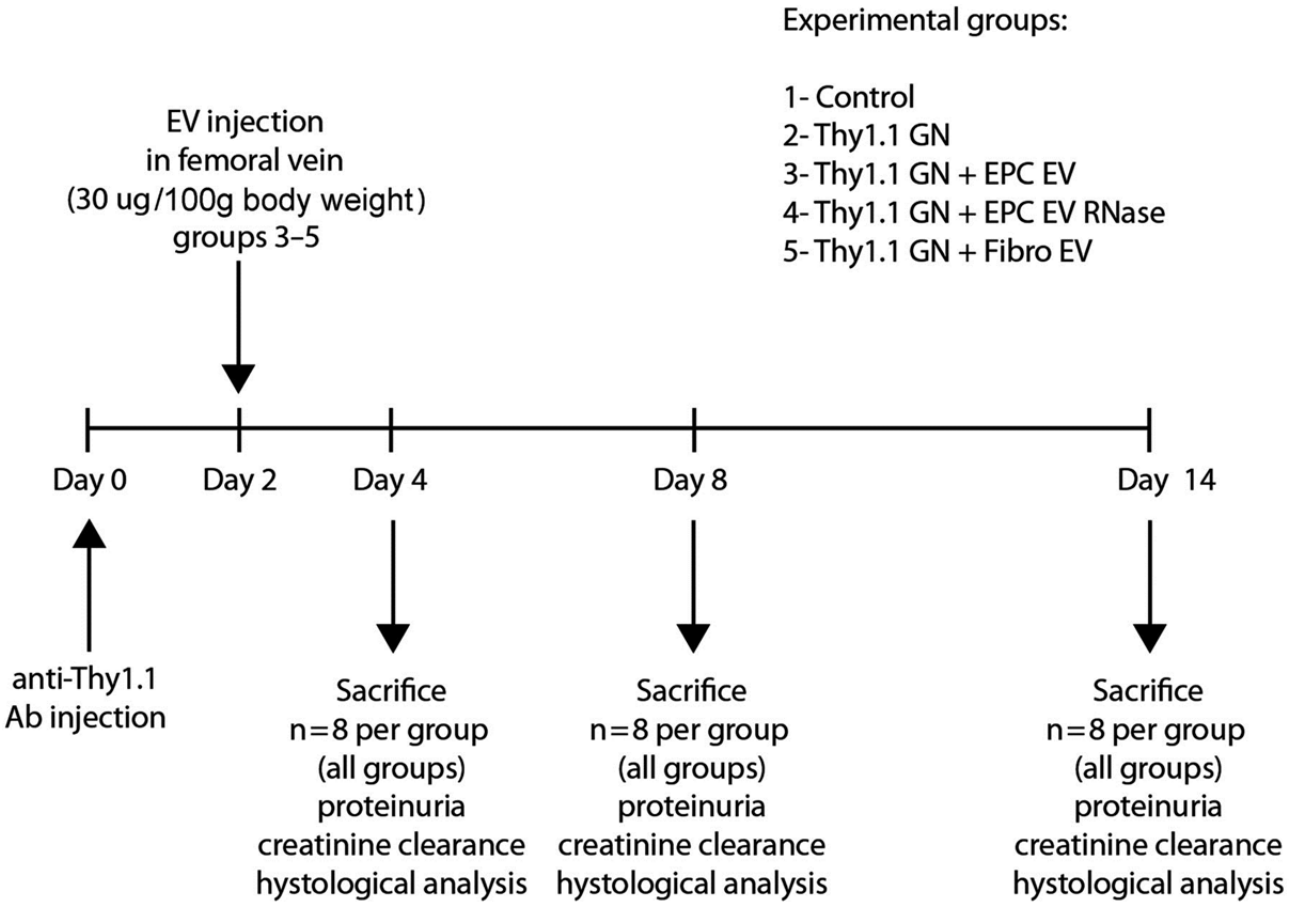

Representative scheme of the experimental plan of anti-Thy1.1 glomerulonephritis in 8-week-old female Wistar rats summarizing experimental groups, number of animals treated (*n* = 8 for each group), modality and dose of EV injection, timing of sacrifice, evaluation of proteinuria/creatinine clearance and histological analysis performed.

FIGURE 3

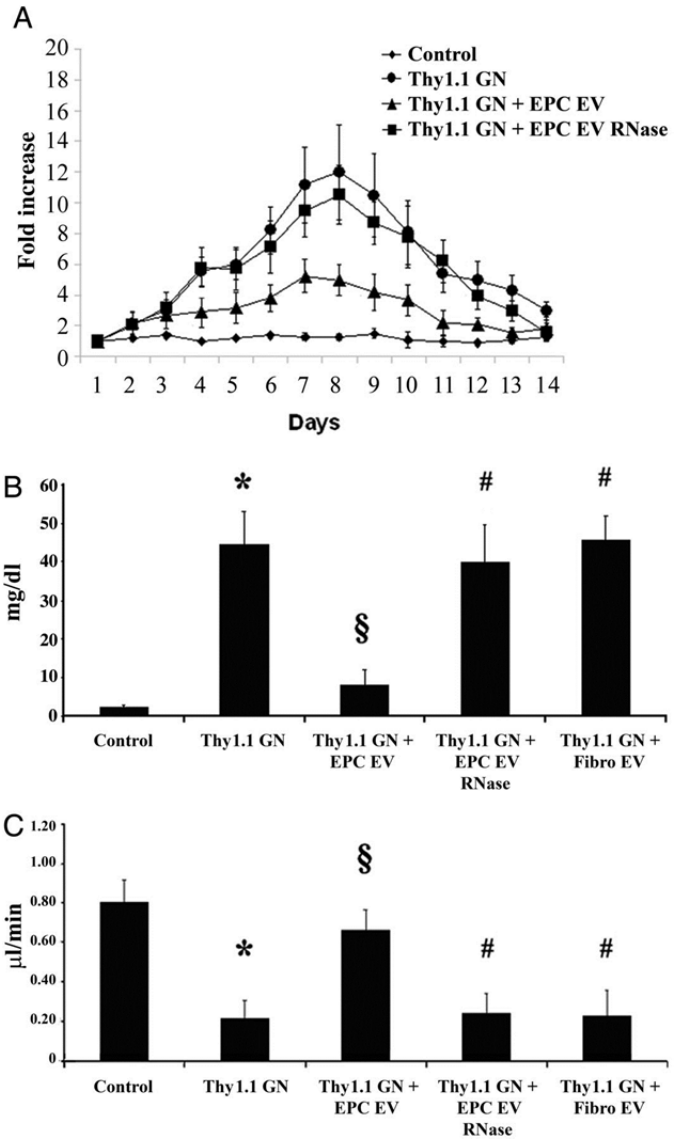

Protective effect of EPC-derived EVs on proteinuria and renal function in anti-Thy1.1 glomerulonephritis. (**A** and **B**) Evaluation of proteinuria expressed as fold increase in respect to basal conditions at different time points (A) or expressed as rough values (mg/dL) at Day 8 (B) in the different experimental groups. Data are expressed as mean ± 1 SD; statistical analysis was performed by ANOVA with Newman–Keuls multicomparison test: *P < 0.05, Thy1.1 GN versus control; §P < 0.05, Thy1.1 GN + EPC EV versus Thy1.1GN; $^{\#}$P < 0.05, Thy1.1 GN + EPC EV RNase or Thy1.1 GN + Fibro EV versus Thy1.1 GN + EPC EV. (**C**) Evaluation of creatinine clearance (µL/min) at Day 8 in the different experimental groups. Data are expressed as mean ± 1 SD; statistical analysis was performed by ANOVA with Newman–Keuls multicomparison test, *P < 0.05, Thy1.1 GN versus control; §P < 0.05 Thy1.1 GN + EPC EV versus Thy1.1GN; $^{\#}$P < 0.05, Thy1.1 GN + EPC EV RNase or Thy1.1 GN + Fibro EV versus Thy1.1 GN + EPC EV. Eight animals for each group were treated with the different experimental conditions.

EPC-derived EVs inhibited glomerular injury decreasing cell death and leucocyte infiltration

Rats treated with anti-Thy1.1 showed at Day 4 the presence of typical early lesions such as mesangiolysis, pre-ballooning, ballooning and loss of microvasculature with formation of pseudoaneurysms and increase of glomerular size (Figure 4A and Table 1). Tubular casts indicated the presence of massive proteinuria (Figure 4A). In respect to controls, the Thy1.1 group showed a significant increase of intraglomerular dead cells detected by TUNEL (Figure 4A and B). EPC-derived EVs inhibited glomerular injury with a significant decrease of histological lesions and of the number of dead cells (Figure 4A and B and Table 1). This protective effect was not observed using RNase-treated EVs (Figure 4A and B and Table 1). Similar results were also observed at Day 8 after EV administration (not shown). The Thy1.1 group showed a massive

infiltration of granulocytes and monocytes at Days 4 and 8. EVs, but not RNase-treated EVs, significantly reduced leucocyte infiltration at both time points (Figure 5A–C).

Table 1. Analysis of glomerular lesions in the different experimental groups

	DAY 4			DAY 8		
Thy1.1	**Thy1.1 + EPC EV**	**Thy1.1 + EPC EV RNase**	**Thy1.1**	**Thy1.1 + EPC EV**	**Thy1.1 + EPC EV RNase**	
Pre-ballooning	12.3 ± 1.2	1.4 ± 0.2	9.5 ± 3.1	32.5 ± 4.2	4.7 ± 1.2	30.2 ± 3.3
Ballooning	3.5 ± 0.9	0.4 ± 0.1	4.2 ± 1.1	16.5 ± 4.1	3.2 ± 1.2	21.7 ± 4.5
Mesangiolysis	74.5 ± 6.2	6.2 ± 1.3	66.6 ± 5.7	26.2 ± 3.6	2.2 ± 0.8	23.2 ± 3.3
Microaneurysms	16.3 ± 2.3	2.3 ± 0.7	21.5 ± 3.1	32.7 ± 4.5	3.8 ± 1.3	36.8 ± 5.1
Podocyte bridging	22.8 ± 3.7	4.3 ± 1.1	18.5 ± 3.2	15.2 ± 2.6	4.2 ± 0.9	16.6 ± 3.1
Tuft adhesion	24.5 ± 4.2	5.5 ± 2.1	27.2 ± 3.6	38.5 ± 4.7	7.7 ± 2.3	36.5 ± 3.8

FIGURE 4

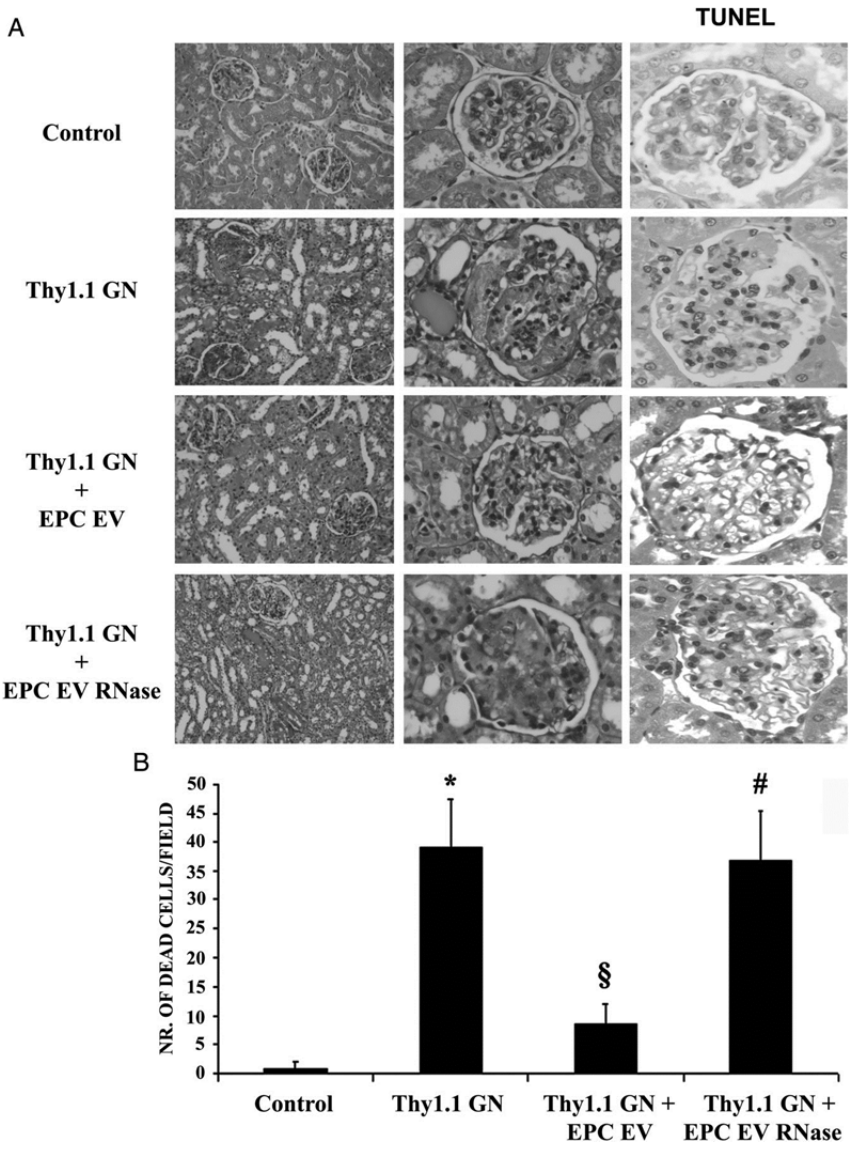

Protective effect induced by EPC-derived EVs on glomerular histological lesions and apoptosis in Thy1.1 glomerulonephritis. (**A**) Representative H&E (×100 magnification in left panels, ×400 magnification in central panels) and TUNEL (×400 magnification in

right panels) staining of kidney sections from different experimental groups at Day 4. (**B**) Count of TUNEL positive cells in different experimental conditions. Data are expressed as mean ± 1 SD. Statistical analysis was performed by ANOVA with Newman–Keuls multicomparison test: *P < 0.05, Thy1.1 GN versus control; §P < 0.05, Thy1.1 GN + EPC EV versus Thy1.1 GN; $^{\#}$P < 0.05, Thy1.1 GN + EPC EV RNase versus Thy1.1 GN + EPC EV. Ten non-consecutive sections for each animal in the different groups were evaluated.

FIGURE 5

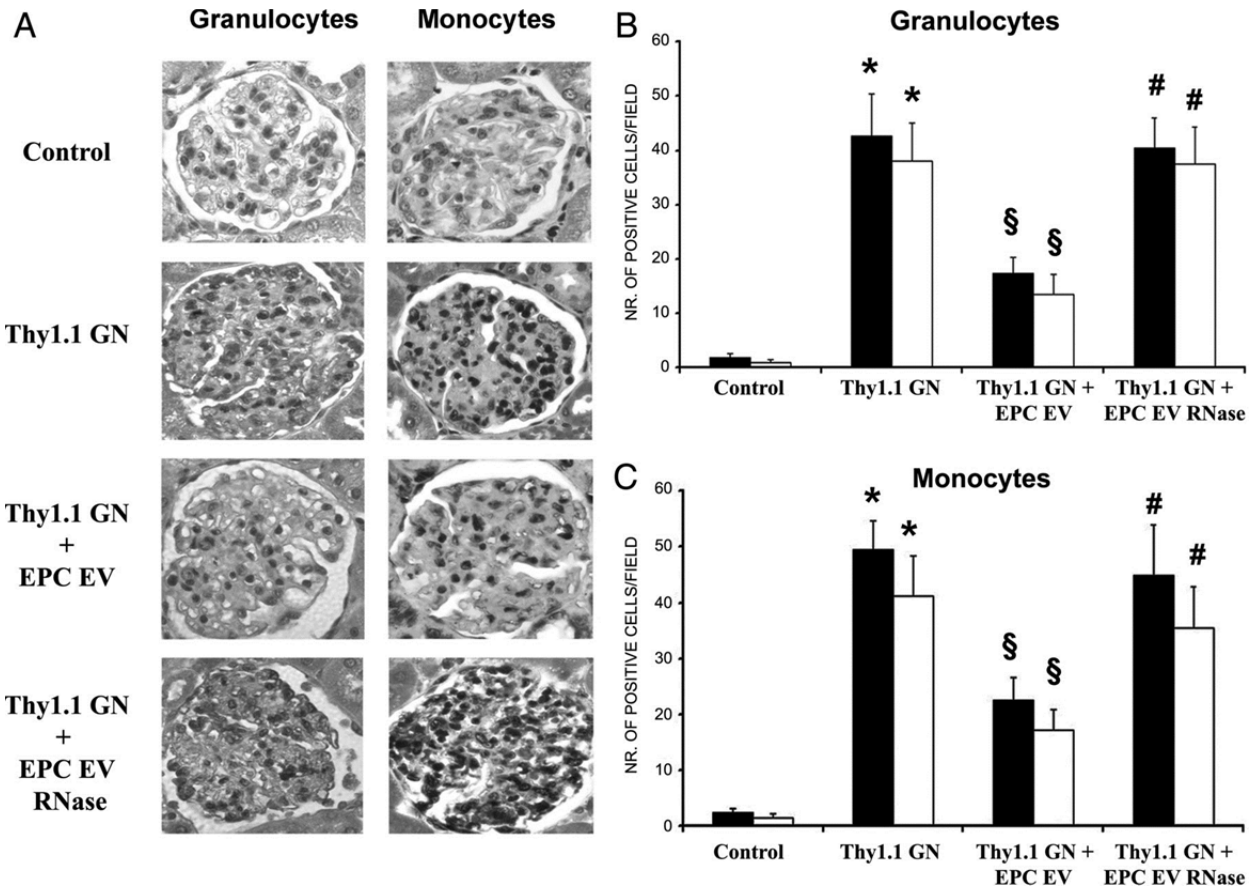

EPC-derived EVs reduced leucocyte infiltration in anti-Thy1.1 glomerulonephritis. (**A**) Representative micrographs (original magnification, ×400) of infiltrating granulocytes and monocytes in different experimental groups at Day 4. (**B** and **C**) Counts of infiltrating granulocytes (B) and monocytes (C) in different experimental groups at Day 4 (black columns) and at Day 8 (white columns). Data are expressed as mean ± 1 SD. Statistical analysis was performed by ANOVA with Newman–Keuls multicomparison test. In respect to control, the Thy1.1 group showed a significant increase of leucocyte infiltration (*P < 0.05, Thy1.1 GN versus control). EVs significantly decreased intraglomerular granulocyte and monocyte infiltration (§P < 0.05, Thy1.1 GN + EPC EV versus Thy1.1 GN). The decrease of leucocyte infiltration was not observed when EVs were treated with RNase ($^{\#}$P < 0.05, Thy1.1 GN + EPC EV RNase versus Thy1.1 GN + EPC EV). Ten non-consecutive sections for each animal in the different groups were evaluated.

EPC-derived EVs preserved glomerular filtration barrier integrity, inhibited mesangial cell C5b-9 deposition and SMA expression and decreased serum complement haemolytic activity (CH50)

Electron microscopy analysis confirmed that endothelial injury, fusion of podocyte foot processes, mesangial cell injury and leucocyte infiltration detected in the Thy1.1 group were inhibited by EPC-derived EVs (Figure 6). As shown by confocal microscopy (Figure 7A), a significant decrease of glomerular staining for RECA-1 and synaptopodin was observed in the Thy1.1 group. EVs preserved the expression of both antigens, suggesting a protective effect on the maintenance of glomerular integrity. In contrast, RNase-treated EVs did not inhibit the loss of RECA-1 and synaptopodin (Figure 7A and Table 2). EVs, but not RNase-treated EVs, significantly reduced the percentage of areas stained for SMA and C5b-9 deposition in the mesangial areas (Figure 7A and Table 2). In comparison to control animals, anti-Thy1.1-treated rats presented a significant decrease of complement haemolytic activity (CH50). In contrast, EVs, but not RNase-treated EVs, increased CH50 activity (Figure 7B).

Table 2. Quantification of RECA-1, synaptopodin and C5b-9 staining and of percentage of SMA positive areas in the different experimental groups

RECA-1 staining FI	Synaptopodin staining FI	Percentage of SMA areas	C5b-9 staining FI	
Control	204.10 ± 31.69	200.97 ± 48.56	0.51 ± 0.77	22.69 ± 12.53
Thy1.1	42.10 ± 28.16	42.04 ± 33.22	32.24 ± 6.15	185.76 ± 47.38
Thy1.1 + EPC EV	156.96 ± 44.78	168.97 ± 56.77	7.56 ± 4.87	41.53 ± 39.99
Thy1.1 + EPC EV RNase	25.50 ± 27.81	38.71 ± 32.44	36.23 ± 3.65	197.91 ± 36.56

FI, Fluorescence intensity (arbitrary units).

FIGURE 6

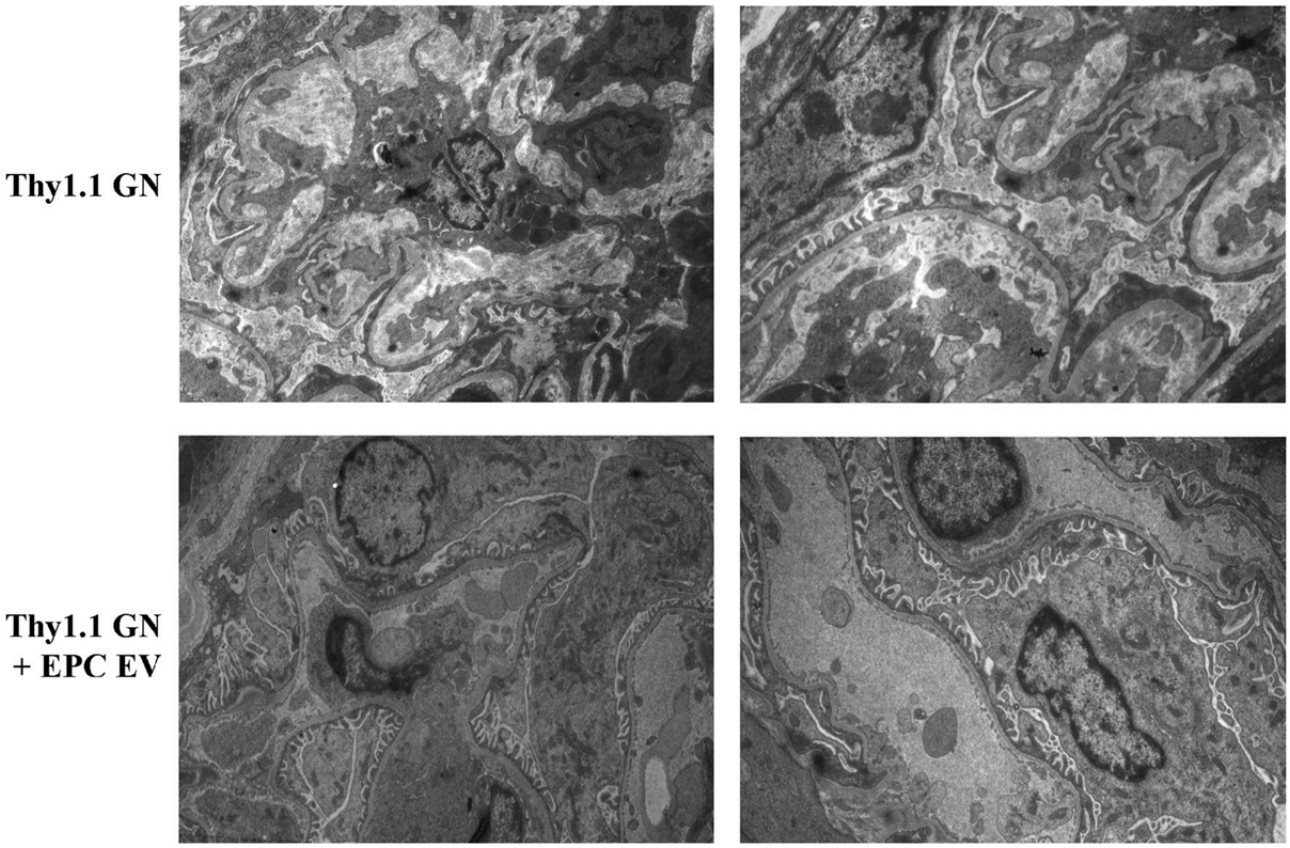

Electron microscopy analysis of kidney sections from rats with Thy1.1 nephritis treated or not with EPC-derived EVs. EVs preserved the integrity of glomerular architecture characterized by a decrease of endothelial injury, fusion of podocyte foot processes and mesangial cell activation. Original magnification was ×7000.

FIGURE 7

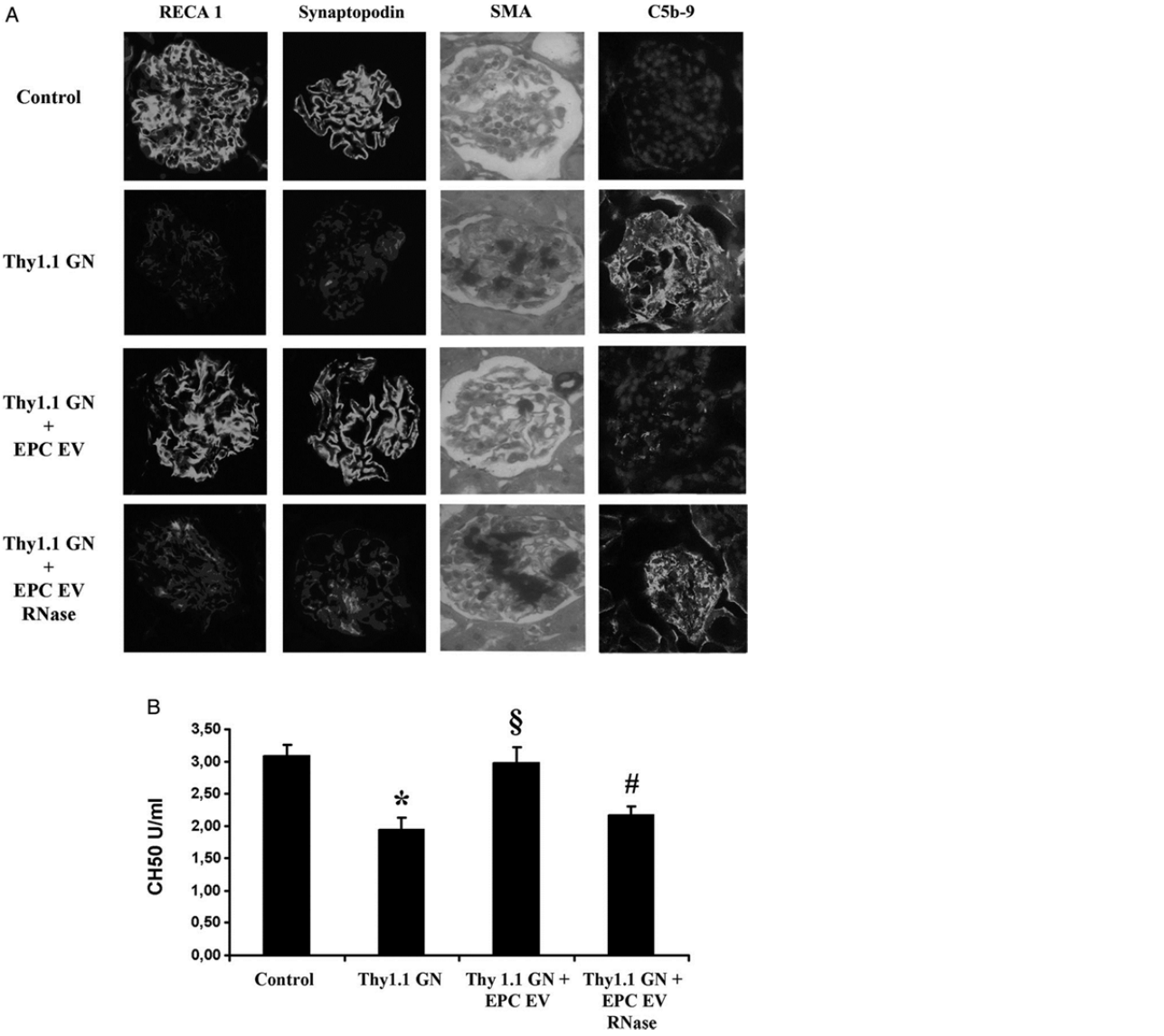

EPC-derived EVs preserved glomerular filtration barrier integrity, inhibited mesangial cell C5b-9 deposition and SMA expression and increased serum complement haemolytic activity (CH50). (**A**) Representative confocal microscope analysis of RECA-1, synaptopodin and C5b-9 and immunoperoxidase staining for SMA in the different experimental groups (original magnification ×400). In confocal microscope micrographs, nuclei were counterstained with 2.5 μg/mL Hoechst. Ten non-consecutive sections for each animal in the different groups were evaluated. (**B**) ELISA evaluation of the complement haemolytic activity (CH50) in sera of rats treated with different experimental conditions. Data are expressed as mean ± 1 SD and statistical analysis was performed by ANOVA with Newman–Keuls multicomparison test: *P < 0.05, Thy1.1 GN versus control; §P < 0.05, Thy1.1 GN + EPC EV versus Thy1.1 GN; $^{\#}$P < 0.05, Thy1.1 GN + EPC EV RNase versus Thy1.1 GN + EPC EV.

Biodistribution and internalization of EPC-derived EVs in glomerular cells

We first evaluated EV biodistribution in healthy animals after i.v. injection. We observed that PKH26 red-labelled EVs mainly localized in the liver 2 h after injection, whereas only few EVs were identified within lung, heart and kidney (Figure 8). We then evaluated EV biodistribution in anti-Thy1.1-treated rats and we found a PKH26 red staining in the liver similar to that observed in untreated animals. However, PKH26-labelled EVs localized into injured glomeruli already 2 h after i.v. injection, particularly in mesangial areas (Figure 9A). Co-staining of red-labelled EVs with RECA-1 and synaptopodin indicated their internalization also in glomerular endothelial and epithelial cells (Figure 9A). The internalization of EVs in RMCs, human mesangial and endothelial cells and podocytes was confirmed *in vitro*. As shown by FACS and confocal

microscopy analysis, EVs were efficiently internalized in all these cell types (Figure 9B). Experiments performed *in vitro* with a blocking antibody directed to L-selectin showed that this molecule played a key role in EV internalization in all glomerular cell types. These results were not observed using an irrelevant isotype-matched mAb (Figure 9C).

FIGURE 8

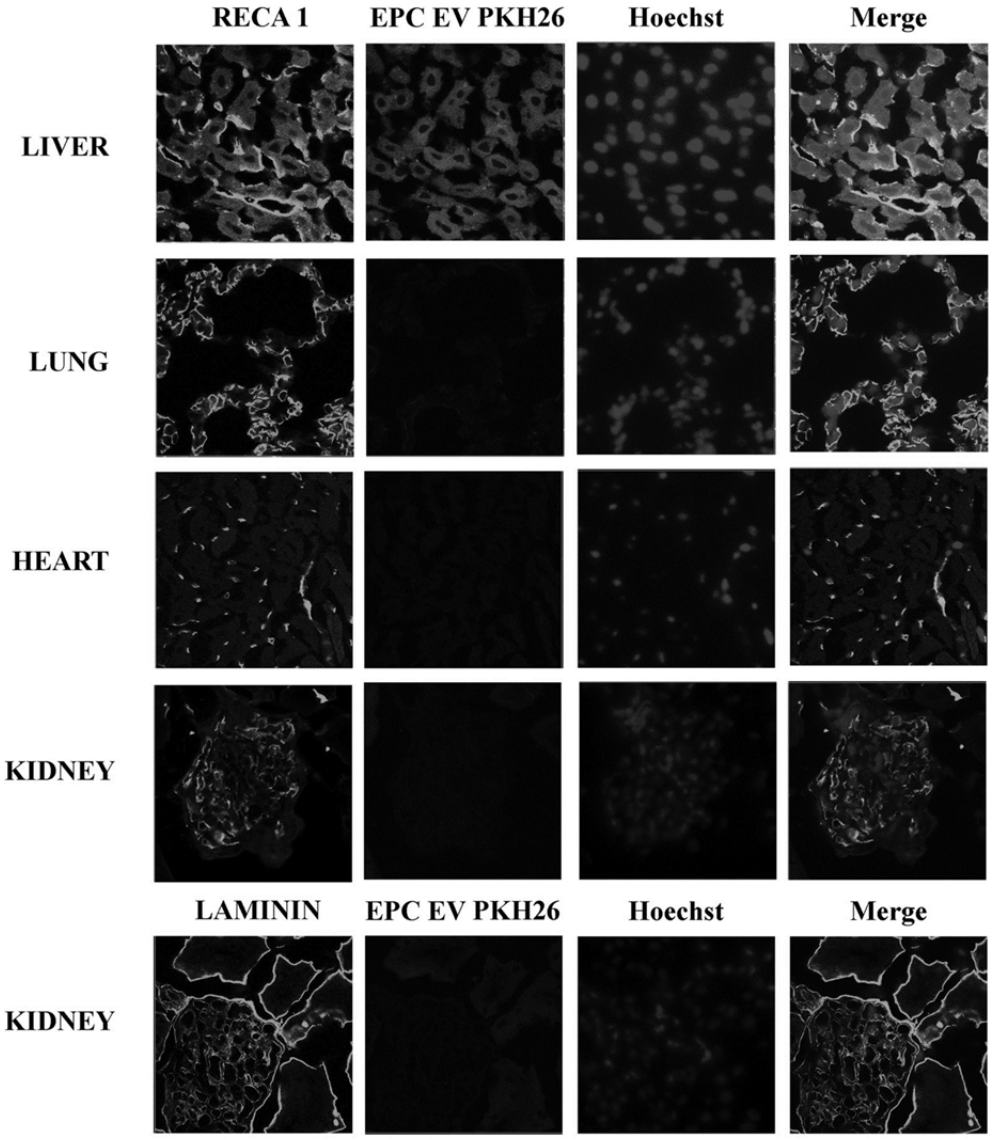

Confocal microscope analysis of biodistribution of EPC-derived EVs in different organs of healthy animals. Representative micrographs showing the co-staining of PKH26 labelled EVs with the endothelial antigen RECA-1 (left panels) in liver, lung, heart and kidney (upper panels). Representative micrographs showing the co-staining of PKH26 red labelled EVs with laminin (left panel) in the kidney (lower panels). In all images, original magnification was ×200, nuclei were counterstained in blue with 2.5 μg/mL Hoechst.

FIGURE 9

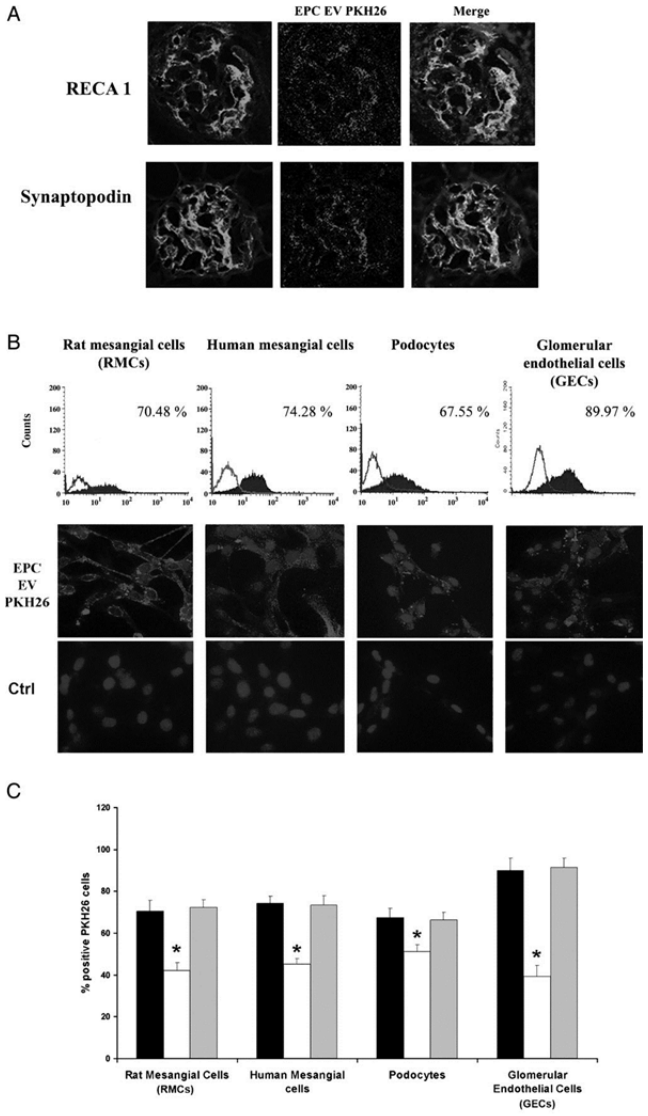

In vivo localization and *in vitro* internalization of EPC-derived EVs in glomerular cells. (**A**) Representative confocal microscope micrographs of PKH26-labelled EVs showing the localization of EVs within glomeruli of anti-Thy1.1-treated animals 2 h after i.v. injection. Co-staining for RECA-1 (upper panels) or for synaptopodin (lower panels) evidenced EV localization within GECs and podocytes, respectively (magnification ×400). In merge images, nuclei were counterstained with 2.5 μg/mL Hoechst. Similar results were observed in six different anti-Thy1.1-treated rats. (**B**) Representative FACS (upper panels) and confocal microscope analysis (lower panels) of PKH26-labelled EVs showing internalization within different glomerular cells *in vitro*. For FACS analysis, control-matched isotype was used as experimental control (open curves). Results are expressed as percentage of red-labelled cells in respect to control. Kolmogorov–Smirnov statistical analysis was performed. In confocal microscope images, magnification was ×400 and nuclei were counterstained with 2.5 μg/mL Hoechst. (**C**) FACS analysis of RMCs, human mesangial cells, human podocytes or human GECs incubated with EPC-derived EVs alone (black column) or in the presence of a blocking mAb directed to L-selectin (white column) or to cytokeratin-19 used as control (gray column). Data are expressed as mean ± 1 SD; statistical analysis was performed by ANOVA with Dunnett's multicomparison test: EV + anti-L-selectin versus EV alone (*$P < 0.05$); EV + anti-cytokeratin-19 versus EV alone (not significant). Three different experiments were performed with similar results.

EPC-derived EVs inhibited complement-mediated RMC injury and C5b-9/C3 deposition *in vitro*

Early observations implied a species-specific action of complement inhibitors. More recent studies challenged this dogma showing that human complement inhibitors Factor H, CD55 and CD59 are not species restricted [22]. To evaluate whether the protective effect of EVs observed *in vivo* in rats could depend on the presence of the human complement inhibitors Factor H, CD55 and CD59, we compared *in*

vitro the detrimental effect of rat and human serum after incubation with EVs. RMCs were incubated with anti-Thy1.1 alone or in the presence of rat or human serum as complement source. Anti-Thy1.1 induced a significant decrease of RMC viability (Figure 10A) and triggered cell death (TUNEL assay in Figure 10B, FACS analysis for annexin V/7-AAD in Figure 10C) when incubated with either rat or human serum [20, 21]. EPC-derived EVs reduced complement-mediated cell damage and death in the presence of either rat or human serum (Figure 10A–C). These effects were not observed when EVs were treated with 1 U/mL RNase or with EVs derived from control human fibroblasts. Incubation with anti-Thy1.1 alone did not change cell viability, whereas incubation with rat or human serum induced cell death but at lower levels to those observed in the presence of both anti-Thy1.1 and serum (Figure 10A–C). In addition, EVs decreased C5b-9 deposition on RMC surface. All these effects were decreased using RNase-treated EVs or EVs derived from human fibroblasts (Figure 11A–C). Incubation with anti-Thy1.1 alone did not change C5b-9 expression, whereas incubation with rat or human serum increased C5b-9 staining but at lower levels to those observed in the presence of both anti-Thy1.1 and serum (Figure 11A–C). Similar results were observed for C3 deposition (Figure 12A–C). As shown by RT-PCR analysis, RMCs incubated with EPC-derived EVs expressed mRNAs coding for the human complement inhibitors Factor H, CD55 and CD59 not detectable in basal conditions or when EVs were pre-treated with RNase (Figure S3, Supplementary Material). These results suggested the putative transfer of mRNAs coding for the complement inhibitors from human EPC-derived EVs to injured RMCs.

FIGURE 10

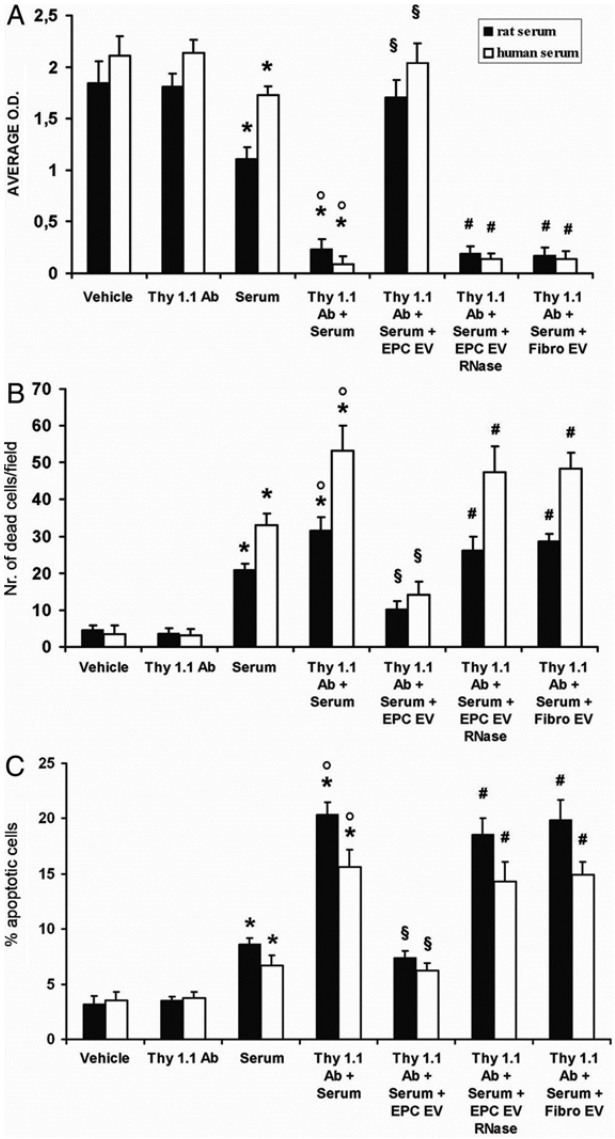

Protective effect of EPC-derived EVs on RMC damage and death induced by anti-Thy1.1 Ab and complement activation. (**A**) XTT-based assay evaluating RMC damage in different experimental conditions. Results are expressed as average optical density (OD) ± 1 SD generated by viable RMCs. (**B**) TUNEL assay showing RMC death in different experimental conditions. Results are expressed as mean number of dead cells ± 1 SD/microscope field (×100 magnification). (**C**) FACS analysis after dual staining with Annexin V and 7-AAD of RMCs treated with different experimental conditions. Results are expressed as percentage of apoptotic cells ± 1 SD. Three experiments were performed with similar results. Statistical analysis was performed by ANOVA with Newman–Keuls multicomparison test. Either 33% rat or human serum induced RMC injury and death (*$P < 0.05$, serum versus vehicle). This effect was significantly enhanced by addition of 4 μg/mL anti-Thy1.1 Ab (*$P < 0.05$, Thy1.1 Ab + serum versus vehicle; °$P < 0.05$ Thy1.1 Ab + serum versus serum alone). EPC EV significantly reduced RMC injury and death ($^{§}P < 0.05$, Thy1.1 Ab + serum + EPC EV versus Thy1.1 Ab + serum). This effect was not observed using RNase-treated EPC EV or fibroblast-derived EV (Fibro EV) ($^{\#}P < 0.05$, Thy1.1 Ab + serum + EPC EV RNase or Fibro EV versus Thy1.1 Ab + serum + EPC EV).

FIGURE 11

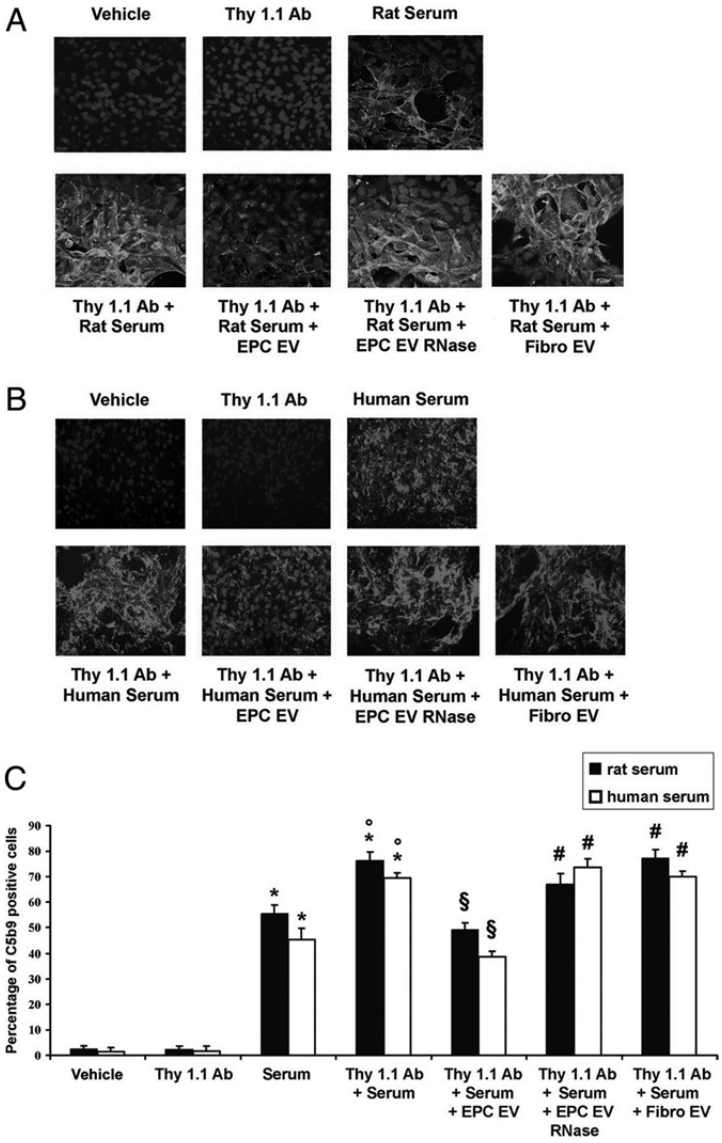

EPC-derived EVs significantly reduced C5b-9 deposition on RMCs. **(A** and **B)** Representative immunofluorescence micrographs of C5b-9 deposition on RMCs treated with different experimental conditions. Rat (A) or human (B) serum was used as complement source, respectively. Three experiments were performed with similar results. Nuclei were counterstained with 2.5 μg/mL Hoechst; original magnification was ×400. (**C**) FACS analysis of C5b-9 deposition on RMCs treated with different experimental conditions. Rat (black columns) or human (white columns) serum was used as complement source, respectively. Statistical analysis was performed by ANOVA with Newman–Keuls multicomparison test. Either 33% rat or human serum induced C5b-9 expression on RMCs (*$P < 0.05$, serum versus vehicle). This effect was significantly enhanced by addition of 4 μg/mL anti-Thy1.1 Ab (*$P < 0.05$, Thy1.1 Ab + serum versus vehicle; °$P < 0.05$, Thy1.1 Ab + serum versus serum alone). EPC EV significantly reduced C5b-9 staining ($^{§}P < 0.05$, Thy1.1 Ab + serum + EPC EV versus Thy1.1 Ab + serum). This effect was not observed using RNase-treated EPC EV or fibroblast-derived EV (Fibro EV) ($^{\#}P < 0.05$, Thy1.1 Ab + serum + EPC EV RNase or Fibro EV versus Thy1.1 Ab + serum + EPC EV).

FIGURE 12

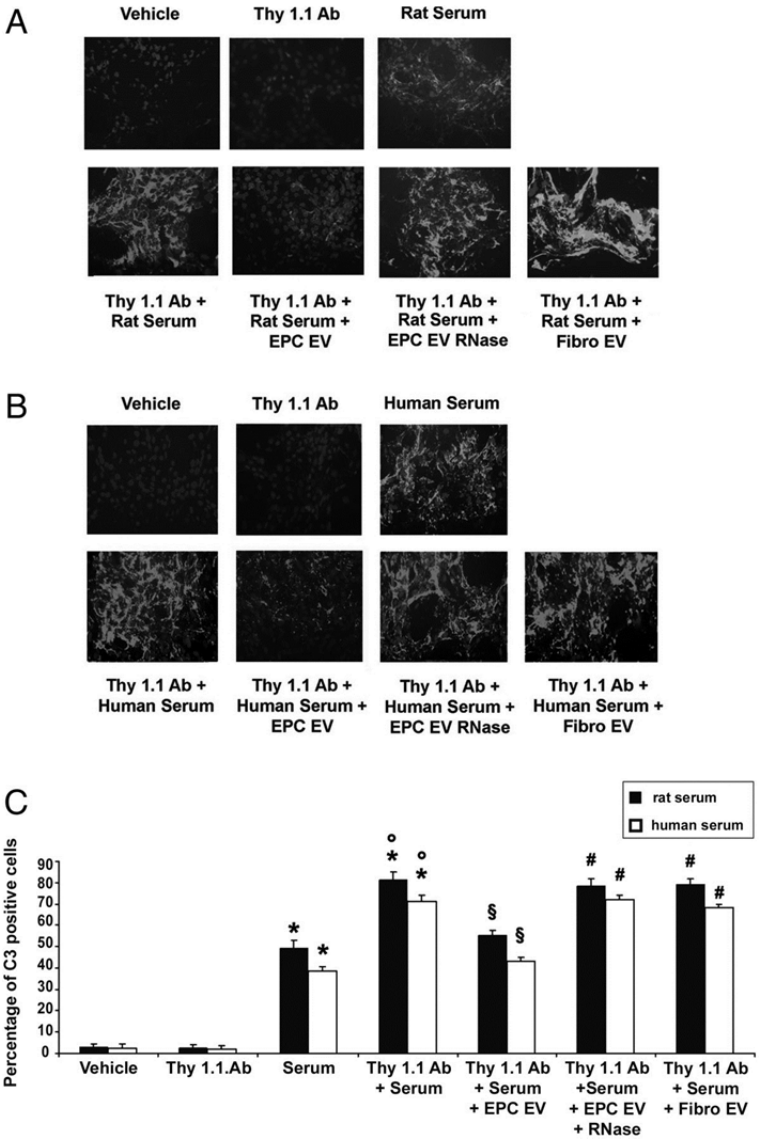

EPC-derived EVs significantly reduced C3 deposition on RMCs. (**A** and **B**) Representative immunofluorescence micrographs of C3 deposition on RMCs treated with different experimental conditions. Rat (A) or human (B) serum was used as complement source, respectively. Three experiments were performed with similar results. Nuclei were counterstained with 2.5 µg/mL Hoechst; original magnification was ×400. (**C**) FACS analysis of C3 deposition on RMCs treated with different experimental conditions. Rat (black columns) or human (white columns) serum was used as complement source, respectively. Statistical analysis was performed by ANOVA with Newman–Keuls multicomparison test. Either 33% rat or human serum induced C3 expression on RMCs (*$P < 0.05$, serum versus vehicle). This effect was significantly enhanced by the addition of 4 µg/mL anti-Thy1.1 Ab (*$P < 0.05$, Thy1.1 Ab + serum versus vehicle; °$P < 0.05$, Thy1.1 Ab + serum versus serum alone). EPC EV significantly reduced C3 staining ($^{§}P < 0.05$, Thy1.1 Ab + serum + EPC EV versus Thy1.1 Ab + serum). This effect was not observed using RNase-treated EPC EV or fibroblast-derived EV (Fibro EV) ($^{\#}P < 0.05$ Thy1.1 Ab + serum + EPC EV RNase or Fibro EV versus Thy1.1 Ab + serum + EPC EV).

DISCUSSION

In this study, we demonstrated that EVs released from bone marrow-derived EPCs inhibit glomerular injury in the experimental model of anti-Thy1.1 mesangiolytic glomerulonephritis. EVs significantly reduced proteinuria, leucocyte infiltration, complement activation and histological lesions such as mesangiolysis, ballooning, rarefaction of microvasculature with formation of pseudoaneurysms and glomerular cell death.

It has been previously shown that in Thy1.1 glomerulonephritis bone marrow-derived EPCs may contribute to inhibit injury, to participate in glomerular endothelial and mesangial cell turnover and to enhance

microvascular repair [5]. EPC-mediated mechanisms of protection from glomerular damage have been mainly ascribed to the release of paracrine mediators such as vasculotrophic growth factors [5, 6]. The EPCs used in this study co-expressed stem cell and endothelial markers typical of the circulating angiogenic progenitor cells but they were negative for monocyte and platelet markers as well as for HLA class I and class II antigens [7, 9, 23, 24]. In addition, EVs expressed on their surface several molecules belonging to the selectin and integrin families that are essential for their internalization and biological activities in target cells [25]. L-selectin was the main adhesion molecule involved in EV entering in the different types of glomerular cells studied.

One of the main findings of this study was that the protective effect of EPC-derived EVs on glomerular injury was specific, because EVs obtained from control human fibroblasts were ineffective. This diversity was accounted to a different genetic content of EVs. We have previously shown that EPC-derived EVs shuttle several mRNAs and microRNAs that can be transferred to injured cells inducing a regenerative programme through the inhibition of apoptosis and the triggering of angiogenesis [7, 9, 26]. Furthermore, we herein described that EPC-derived EVs but not fibroblast-derived EVs carried mRNA coding for the complement inhibitors Factor H, CD55 and CD59 as well as the correspondent proteins. Complement Factor H is a key regulator of the alternative pathway whose deficiency is associated with different human diseases including haemolytic uraemic syndrome, membranoproliferative glomerulonephritis, lupus nephritis and transplant rejection [27, 28]. The lack of Factor H leads to a massive C3 activation with consequent accumulation in the glomerular structures. The treatment with human Factor H has been shown to reverse renal complement deposition in Factor H-deficient mice [29]. CD55 or decay-accelerating factor (DAF) is a complement regulator widely expressed in mammalian tissues which is known to inhibit the classical and the alternative pathways by targeting C3 convertase. CD55 deficiency leads to an increased susceptibility to develop anti-glomerular basement membrane nephritis or focal and segmental glomerulosclerosis [30, 31]. In acute toxic nephritis, CD55 has been shown to confer protection from complement-mediated podocyte injury [32]. CD59 is a regulatory protein that inhibits C5b-9, the terminal effector of cell damage able to trigger glomerular cell death [32, 33]. Several studies demonstrated that complement activation mediates the typical histological lesions of experimental Thy1.1 glomerulonephritis. In particular, the mesangial injury has been ascribed to cell death consequent to C5b-9 formation. Indeed, C5b-9 has been shown to induce the release of mediators able to worsen mesangial cell damage such as inflammatory cyotokines and nitric oxide [34]. Moreover, C5b-9 can trigger mesangial cell apoptosis via a caspase-dependent manner [35]. In this study, we observed a reduced deposition of C5b-9 within glomeruli of rats treated with EVs. This could depend on the reduced accumulation of inflammatory cells and/or on the delivery of inhibitors of complement activation by EVs. The Factor H, CD55 and CD59 complement inhibitors carried by EPC-derived EVs are of human origin and therefore according to the dogma of species specificity action of complement inhibitors should not be active in rats. However, this dogma has been recently challenged as it has been shown that there is considerable cross-species activity for these membrane regulators of complement activation [22]. Studies aimed to investigate the capacity of human, rat and mouse analogues of CD55 to regulate homologous and heterologous complement activation revealed the absence of species restriction [22, 36]. Similar results were observed for CD59 [22, 37]. In this study, we compared the ability of human EPC-derived EVs to inhibit *in vitro* Thy1.1-induced RMC injury in the presence of rat or human serum as complement source. The inhibitory effect of EVs on mesangial cell injury was observed not only using rat but also human serum. Therefore, the results of this study suggest that the protective effect of EPC-derived EVs may depend on the transfer of mRNAs coding for the human complement inhibitors Factor H, CD55 and CD59 as well as the correspondent proteins to injured RMCs. This transfer resulted in a significant reduction of C5b-9 and C3 deposition and consequent complement-mediated cell injury. Moreover, the expression of SMA by mesangial cells was inhibited by EPC-derived EVs, suggesting a limitation of myofibroblastic differentiation. The loss of the protective effect of EVs both *in vivo* and *in vitro* after RNAse treatment further suggests that the biological effects of EVs are mainly related to the transfer of RNAs.

In conclusion, EVs released from EPCs decrease proteinuria and inhibit glomerular injury by transferring specific RNAs in experimental anti-Thy1.1 glomerulonephritis. This protective effect may depend on the

limitation of cell death and inflammatory cell recruitment induced by antibody- and complement-mediated injury of mesangial cells.

REFERENCES

1. Nakamura K, Oka M, Shirai M, et al. Source of reactive oxygen species in anti-Thy1 nephritis. Ren Fail 1998;20:399-405.
2. Kunter U, Rong S, Djuric Z, et al. Transplanted mesenchymal stem cells accelerate glomerular healing in experimental glomerulonephritis. J Am Soc Nephrol 2006;17:2202-2212.
3. Rampino T, Gregorini M, Bedino G, et al. Mesenchymal stromal cells improve renal injury in anti-Thy 1 nephritis by modulating inflammatory cytokines and scatter factors. Clin Sci 2011;120:25-36.
4. Zampetaki A, Kirton JP, Xu Q. Vascular repair by endothelial progenitor cells. Cardiovasc Res 2008;78:413-421.
5. Uchimura H, Marumo T, Takase O, et al. Intrarenal injection of bone marrow-derived angiogenic cells reduces endothelial injury and mesangial cell activation in experimental glomerulonephritis. J Am Soc Nephrol 2005;16:997-1004.
6. Yang Z, von Ballmoos MW, Faessler D, et al. Paracrine factors secreted by endothelial progenitor cells prevent oxidative stress-induced apoptosis of mature endothelial cells. Atherosclerosis 2010;211:103-109.
7. Deregibus MC, Cantaluppi V, Calogero R, et al. Endothelial progenitor cell derived microvesicles activate an angiogenic program in endothelial cells by a horizontal transfer of mRNA. Blood 2007;110:2440-2448.
8. Ratajczak J, Wysoczynski M, Hayek F, et al. Membrane-derived microvesicles: important and underappreciated mediators of cell-to-cell communication. Leukemia 2006;20:1487-1495.
9. Cantaluppi V, Gatti S, Medica D, et al. Microvesicles derived from endothelial progenitor cells protect the kidney from ischemia-reperfusion injury by microRNA-dependent reprogramming of resident renal cells. Kidney Int 2012;82:412-427.
10. Théry C, Regnault A, Garin J, et al. Molecular characterization of dendritic cell-derived exosomes. Selective accumulation of the heat shock protein hsc73. J Cell Biol 1999;147:599-610.
11. Figliolini F, Cantaluppi V, De Lena M, et al. Isolation, characterization and potential role in Beta cell-endothelium cross-talk of extracellular vesicles released from human pancreatic islets. PLoS One 2014;9:e102521.
12. Kriz W, Hähnel B, Hosser H, et al. Pathways to recovery and loss of nephrons in anti Thy-1 nephritis. J Am Soc Nephrol 2003;14:1904-1926.
13. Bussolati B, Bruno S, Grange C, et al. Isolation of renal progenitor cells from adult human kidney. Am J Pathol 2005;166:545-555.
14. Conaldi PG, Bottelli A, Baj A, et al. Human immunodeficiency virus-1 tat induces hyperproliferation and dysregulation of renal glomerular epithelial cells. Am J Pathol 2002;161:53-61.
15. Conaldi PG, Bottelli A, Wade-Evans A, et al. HIV-persistent infection and cytokine induction in mesangial cells: a potential mechanism for HIV-associated glomerulosclerosis. AIDS 2000;14:2045-2047.

16. Nauta AJ, Daha MR, Tijsma O, et al. The membrane attack complex of complement induces caspase activation and apoptosis. Eur J Immunol 2002;32:783-792.
17. Cantaluppi V, Biancone L, Romanizzi GM, et al. Macrophage stimulating protein may promote tubular regeneration after acute injury. J Am Soc Nephrol 2008;19:1904-1918.
18. Bruno S, Grange C, Collino F, et al. Microvesicles derived from mesenchymal stem cells enhance survival in a lethal model of acute kidney injury. PLoS One 2012;7:e33115.
19. Cantaluppi V, Weber V, Lauritano C, et al. Protective effect of resin adsorption on septic plasma-induced tubular injury. Crit Care 2010;14:R4.
20. Cragg MS, Howatt WJ, Bloodworth L, et al. Complement mediated cell death is associated with DNA fragmentation. Cell Death Differ 2000;7:48-58.
21. Golay J, Introna M. Mechanism of action of therapeutic monoclonal antibodies: promises and pitfalls of in vitro and in vivo assays. Arch Biochem Biophys 2012;526:146-153.
22. Morgan BP, Berg CW, Harris CL. 'Homologous restriction' in complement lysis: roles of membrane complement regulators. Xenotransplantation 2005;12:258-265.
23. Prokopi M, Pula G, Mayr U, et al. Proteomic analysis reveals presence of platelet microparticles in endothelial progenitor cell cultures. Blood 2009;114:723-732.
24. Yoon CH, Hur J, Park KW, et al. Synergistic neovascularization by mixed transplantation of early endothelial progenitor cells and late outgrowth endothelial cells: the role of angiogenic cytokines and matrix metalloproteinases. Circulation 2005;112:1618-1627.
25. Biancone L, Cantaluppi V, Duò D, et al. Role of L-selectin in the vascular homing of peripheral blood-derived endothelial progenitor cells. J Immunol 2004;173:5268-5274.
26. Cantaluppi V, Biancone L, Figliolini F, et al. Microvesicles derived from endothelial progenitor cells enhance neoangiogenesis of human pancreatic islets. Cell Transplant 2012;21:1305-1320.
27. Noris M, Remuzzi G. Translational mini-review series on complement factor H: therapies of renal diseases associated with complement factor H abnormalities: atypical haemolytic uraemic syndrome and membranoproliferative glomerulonephritis. Clin Exp Immunol 2008;151:199-209.
28. Bao L, Haas M, Quigg RJ. Complement factor H deficiency accelerates development of lupus nephritis. J Am Soc Nephrol 2011;22:285-295.
29. Fakhouri F, de Jorge EG, Brune F, et al. Treatment with human complement factor H rapidly reverses renal complement deposition in factor H-deficient mice. Kidney Int 2010;78:279-286.
30. Sogabe H, Nangaku M, Ishibashi Y, et al. Increased susceptibility of decay-accelerating factor deficient mice to anti-glomerular basement membrane glomerulonephritis. J Immunol 2001;167:2791-2797.
31. Bao L, Haas M, Pippin J, et al. Focal and segmental glomerulosclerosis induced in mice lacking decay-accelerating factor in T cells. J Clin Invest 2009;119:1264-1274.
32. Lin F, Salant DJ, Meyerson H, et al. Respective roles of decay-accelerating factor and CD59 in circumventing glomerular injury in acute nephrotoxic serum nephritis. J Immunol 2004;172:2636-2642.
33. Huang Y, Qiao F, Abagyan R, et al. Defining the CD59-C9 binding interaction. J Biol Chem 2006;281:27398-27404.
34. Lovett DH, Haensch GM, Goppelt M, et al. Activation of glomerular mesangial cells by the terminal membrane attack complex of complement. J Immunol 1987;138:2473-2480.

35. Liu L, Qiu W, Wang H, et al. Sublytic C5b-9 complexes induce apoptosis of glomerular mesangial cells in rats with Thy-1 nephritis through role of interferon regulatory factor-1-dependent caspase 8 activation. J Biol Chem 2012;287:16410-16423.
36. Harris CL, Spiller OB, Morgan BP. Human and rodent decay-accelerating factors (CD55) are not species restricted in their complement-inhibiting activities. Immunology 2000;100:462-470.
37. Powell MB, Marchbank KJ, Rushmere NK, et al. Molecular cloning, chromosomal localization, expression, and functional characterization of the mouse analogue of human CD59. J Immunol 1997;158:1692-1702.